Auger recombination in HgCdTe quantum wires and quantum boxes

Y. Jiang, M. C. Teich, and W. I. Wang
Department of Electrical Engineering, Columbia University, New York, New York 10027

J. R. Meyer
Naval Research Laboratory, Washington, DC 20375

(Received 10 July 1991; accepted for publication 20 December 1991)

Quantum-wire and quantum-box structures for narrow-gap materials with small effective masses, such as HgCdTe, can readily be fabricated using current lithographic techniques. In this article, we calculate the Auger-recombination carrier lifetimes in HgCdTe quantum-wire and quantum-box structures, with band gaps in the 2–5 μm wavelength range. Quantum confinement is generally believed to increase the carrier lifetimes. However, we find the Auger recombination lifetime in a HgCdTe quantum wire is shorter than that in a quantum well, and it decreases as the wire width decreases because of the corresponding increase in the density of states. On the other hand, band-to-band Auger recombination is zero in a quantum box because the overlap functions vanish and because of the discrete nature of the energy levels. Therefore, within the confines of our model, we can expect improved temperature performance from long-wavelength quantum-box lasers but not from quantum-wire lasers. Furthermore, these conclusions are applicable for all types of band-to-band Auger processes and semiconductor materials.

I. INTRODUCTION

There has been increasing interest in developing semiconductor lasers that operate in the 2–5 μm wavelength range.[1,2] These lasers have already found application in high-resolution gas spectroscopy, air-pollution monitoring, and infrared heterodyne detection.[1] They have potential applications in communication systems utilizing fluoride glass fibers,[3] which have minimal losses in the 2–4 μm wavelength region. The intrinsic losses in glass fibers arise from Rayleigh scattering, which decreases as $1/\lambda^4$ as the wavelength increases.[4] With highly developed fluoride glass fibers the transmission losses in a communication system can be substantially reduced, and efficient lasers operating in this wavelength range would be required.[5]

There has been extensive research on these lasers.[6–8] However, because of the dominance of Auger recombination in carrier losses, the threshold current for lasing increases and the internal quantum efficiency decreases so rapidly with increasing temperature that their performance is impaired as the temperature increases. Quantum confinement is generally believed to increase the carrier lifetimes.[9,10] In this article, we investigate how a one-dimensional structure—the quantum wire (QWR)—and a zero-dimensional structure—the quantum box (QB)—affect Auger recombination. We consider narrow-gap HgCdTe as an example of interest because its small effective mass enables us to make quantum confinement structures of sufficiently large dimensions that they can be fabricated using current lithographic techniques.

II. LIMIT OF QUANTUM CONFINEMENT

In order for quantum effects to be perceptible in a confined structure, the linear dimension d has to be smaller than the carrier mean free path. The carrier mean free path in a compound semiconductor is determined by the longitudinal-optical (LO) phonon scattering rate, which is given (in CGS unit) by[11]

$$1/\tau_{\mathrm{LO}} = F(m^*)^{1/2}, \tag{1}$$

with

$$F = 2\left(\frac{1}{\epsilon_\infty} - \frac{1}{\epsilon_0}\right)\left(\frac{q^4\omega_{\mathrm{LO}}}{2\hbar^3}\right)^{1/2} \frac{1}{e^{\hbar\omega_{\mathrm{LO}}/k_BT} - 1}, \tag{2}$$

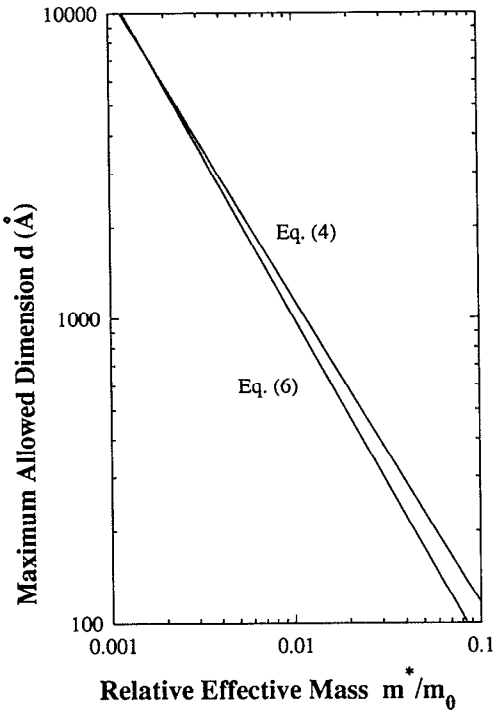

FIG. 1. The maximum allowed value of d vs the relative effective mass m^* for HgCdTe at room temperature. The upper curve is calculated from Eq. (4), and the lower curve is calculated according to Eq. (5).

 0021-8979/92/073394-05$04.00

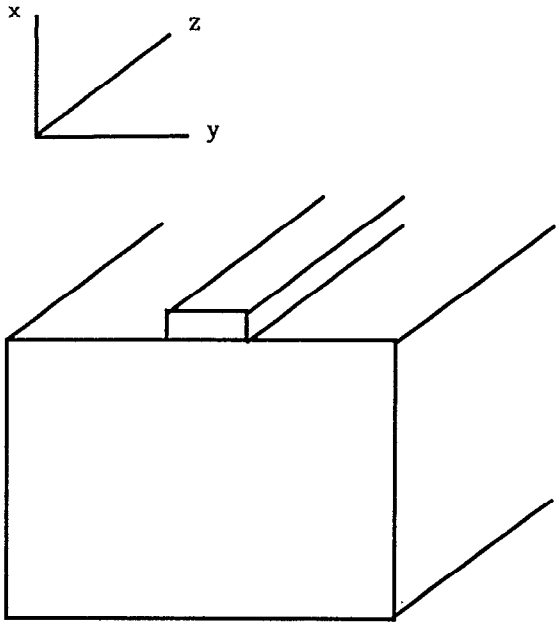

FIG. 2. A quantum-wire structure.

where $\hbar\omega_{LO}$ is the LO phonon energy $\approx$10–40 meV in II-VI semiconductors, ϵ_∞ and ϵ_0 are the optical and static dielectric constants, q is the electron charge, k_B is the Boltzmann constant, and T is the temperature.

The average velocity of a carrier in the well is $\sqrt{2k_BT/m^*}$. Therefore, if the well width is narrow enough,

$$d < \sqrt{\frac{2k_BT}{m^*}}\,\tau_{LO}, \tag{3}$$

the carriers are not likely to experience phonon scattering across the entire width. According to Eqs. (1) and (3)

$$d < \frac{\sqrt{2k_BT}}{F}\,(m^*)^{-1}. \tag{4}$$

To be more realistic, the LO phonon scattering lifetime can be obtained from the following empirical expression for the mobility of narrow-gap HgCdTe,

$$\mu_n = \frac{q\tau_{LO}}{m^*} = 12.9\left(\frac{m^*}{m_0}\right)^{-1.58}\ (\mathrm{cm^2/s\ V}). \tag{5}$$

Therefore

$$d < \sqrt{2k_BT}\,\frac{\mu_n}{q}\,(m^*)^{0.5}. \tag{6}$$

The maximum allowed value of d versus the relative effective mass for HgCdTe at room temperature is shown in Fig. 1, assuming an LO phonon energy of 10 meV.[12] The upper curve is the result of Eq. (4), and the lower curve, which is reduced by about 50%, is the result according to Eq. (6). Other parameters are the same as those used in Ref. 13. For $Hg_{0.65}Cd_{0.35}Te$, $m_c = 0.025m_0$, $E_g = 0.36$ eV, and the maximum value of d is about 370 Å; for $Hg_{0.85}Cd_{0.15}Te$, $m_c = 0.006m_0$, $E_g = 0.084$ eV, and the maximum value of d is about 1700 Å. At the current state of technology, it is not an easy task to make QWR or QB structures of 300 Å lateral dimension. However, structures of 1000 Å are within reach. In these structures, the electrons are in states of quantum confinement, but the holes may not be because of their larger masses. However, as we will see in Sec. III, the holes can only be in certain states to participate in an Auger process because of the conservation of momentum and energy. Therefore, for the purpose of comparing the Auger recombination lifetimes in QW, QWR, and QB structures, we may approximate that the holes are in states of quantum confinement as well.

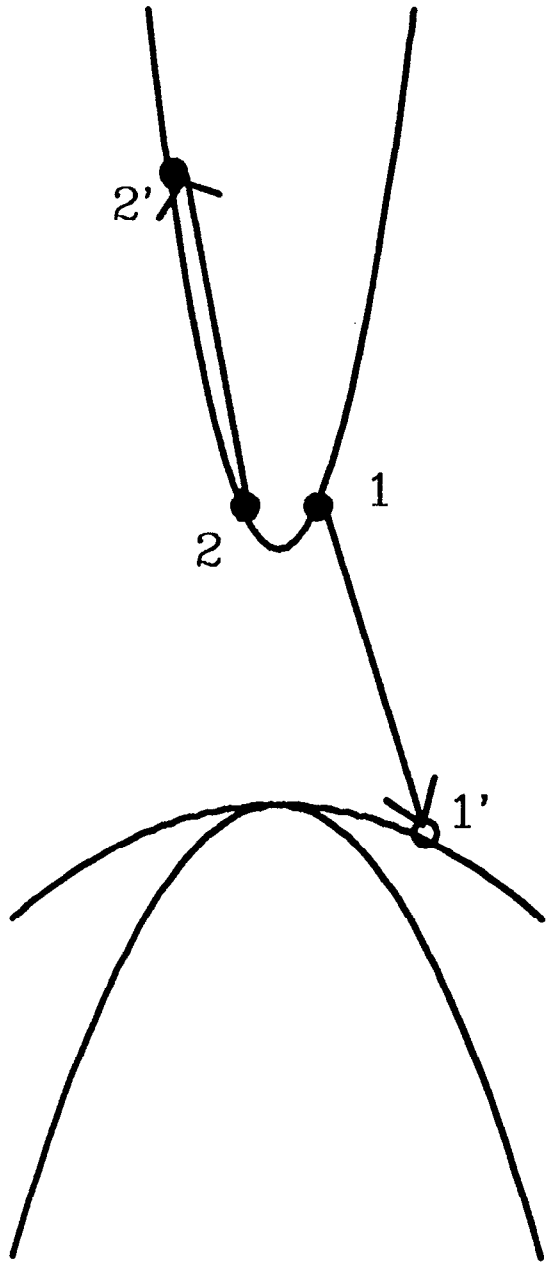

FIG. 3. The CCCH Auger process.

III. CCCH AUGER RECOMBINATION IN QUANTUM WIRES

In a quantum wire (Fig. 2) with infinitely high barriers, the carriers are confined in the x and y directions, and the set of eigenfunctions $\varphi_{i,m,n}$ can be written as

$$\phi_{i,m,n} = u_{i,k}(\mathbf{r}) e^{-ikz} \sqrt{\frac{4}{d_x d_y}} \sin(\xi_m x) \sin(\xi_n y), \qquad (7)$$

where u is the periodic part of the Bloch function, $\mathbf{r} = (x,y,z)$ is the position vector of the carrier, k is the wave vector along the wire length (z direction), d_x and d_y are the widths along the x and y direction, and

$$\xi_m = m\frac{\pi}{d_x}, \quad m = 1,2,\ldots; \quad \text{and} \quad \xi_n = n\frac{\pi}{d_y}, \quad n = 1,2,\ldots . \qquad (8)$$

Band-to-band Auger recombination in narrow-gap HgCdTe is dominated by the CCCH process,[14,15] in which, as shown in Fig. 3, a conduction-band electron 1 (C) recombines with a heavy hole 1′ (H), exciting an electron 2 (C) to the state 2′ (C) of higher energy.

The one-dimensional CCCH Auger recombination rate per unit volume R_{Aug} ($\mathrm{cm}^{-3}\,\mathrm{s}^{-1}$) can be written as[13]

$$R_{\mathrm{Aug}} = \frac{2\pi}{h}\left(\frac{1}{2\pi}\right)^3 \frac{1}{(d_x d_y)^3} \times \sum_{\substack{\xi_{ix},\xi_{x1},\xi_{x1'},\xi_{x2},\xi_{x2'};\\ \xi_{y},\xi_{y1},\xi_{y1'},\xi_{y2},\xi_{y2'}}} \iiiint dk_1\, dk_2\, dk_{1'}\, dk_{2'} \times |M_A|^2 P(1,1',2,2') \delta(k_1 + k_2 - k_{1'} - k_{2'}) \times \delta(E_f - E_i), \qquad (9)$$

where the k's are carrier wave vectors, E_i and E_f are the initial and final energies of the process, respectively, and

$$E_f - E_i = E(1') + E(2') - E(1) - E(2). \qquad (10)$$

Neglecting exchange terms, the matrix element is

$$|M_A|^2 = 4\left(\frac{4\pi q^2}{\epsilon}\right)^2 \left|\frac{F_{1,1'}F_{2,2'}G_{1,1'}(\xi_x)G_{2,2'}(-\xi_x)G_{1,1'}(\xi_y)G_{2,2'}(-\xi_y)}{(k_{2'}-k_2)^2 + \xi_x^2 + \xi_y^2 + \lambda^2}\right|^2, \qquad (11)$$

where

$$G_{i,j}(\xi) = \tfrac{1}{2}(\delta_{\xi,\xi_i-\xi_j} + \delta_{\xi,\xi_j-\xi_i} - \delta_{\xi,\xi_i+\xi_j} - \delta_{\xi,-\xi_i-\xi_j}), \qquad (12)$$

q, ϵ, and λ are the electron charge, static dielectric constant, and screening factor, respectively, and $|F_{ij}|^2$ are the overlap functions.[16] The quantity $P(1,1',2,2')$, taking the reverse process of CCCH Auger recombination into account also, represents the occupation probabilities. Assuming that the electron and hole distributions f_n and f_p can be expressed as Fermi distributions, with electron and hole quasi-Fermi levels F_n and F_p, respectively, we have

$$\begin{aligned} P(1,1',2,2') &= f_n(\mathbf{k}_1) f_n(\mathbf{k}_2) f_p(\mathbf{k}_{1'}) [1 - f_n(\mathbf{k}_{2'})] \\ &\quad - [1 - f_n(\mathbf{k}_1)][1 - f_n(\mathbf{k}_2)] \\ &\quad \times [1 - f_p(\mathbf{k}_{1'})] f_n(\mathbf{k}_{2'}) \\ &= \{1 - \exp[-(F_n - F_p)/k_B T]\} \\ &\quad \times f_n(\mathbf{k}_1) f_n(\mathbf{k}_2) f_p(\mathbf{k}_{1'}) [1 - f_n(\mathbf{k}_{2'})]. \end{aligned} \qquad (13)$$

The $G_{ij}(\xi)$'s impose selection rules on the summations. Equation (9) can be reduced to a third-order integration as described in Ref. 13.

If the Fermi levels are sufficiently away from the band edges, Eq. (9) can be approximated as

$$R_{\mathrm{Aug}} = Cpn^2, \qquad (14)$$

where n and p are the electron and hole concentrations, respectively, and the constant C is called the Auger recombination constant. For intrinsic semiconductors, and for semiconductors with high levels of carrier injection, which is the case in semiconductor lasers, $n = p$. The Auger recombination lifetime, defined as

$$\tau = p/R_{\mathrm{Aug}}, \qquad (15)$$

is a measure that is often used to characterize the performance of semiconductor lasers.

If we assume the bands are parabolic, the calculation of Eq. (9) can be simplified. Although this approximation introduces errors in the absolute values of the calculated recombination rates, it is adequate for comparing the Auger recombination rates in HgCdTe quantum-wire and quantum-well structures. A more accurate calculation of the bands is illustrated in Ref. 17. Figure 4 shows the Auger recombination lifetime τ in $Hg_{0.65}Cd_{0.35}Te$ QWRs for various values of the wire width. We can see that the recombination time is shorter in a QWR than in a quantum well (QW) and decreases with decreasing wire width. This

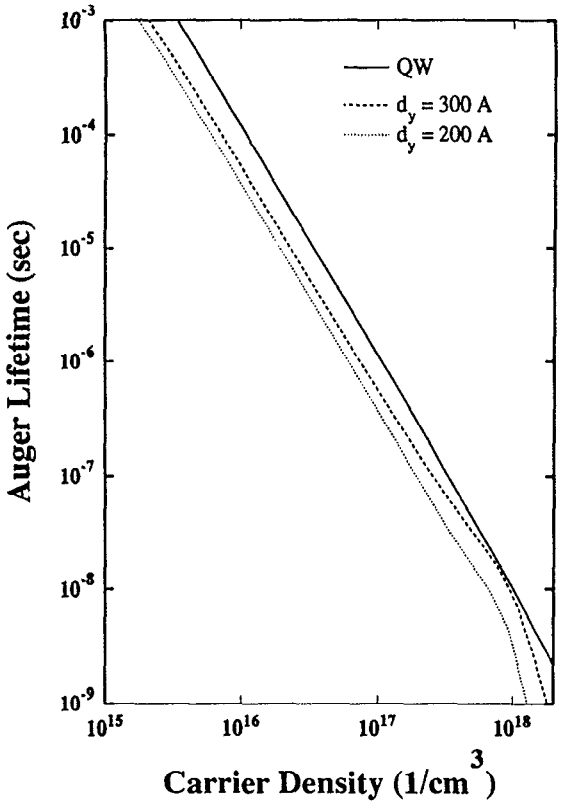

FIG. 4. Auger recombination lifetime in $Hg_{0.65}Cd_{0.35}Te$ QWRs of $d_x = 200$ Å and various values of d_y and a quantum well (d_y is infinite) at $T = 300$ K.

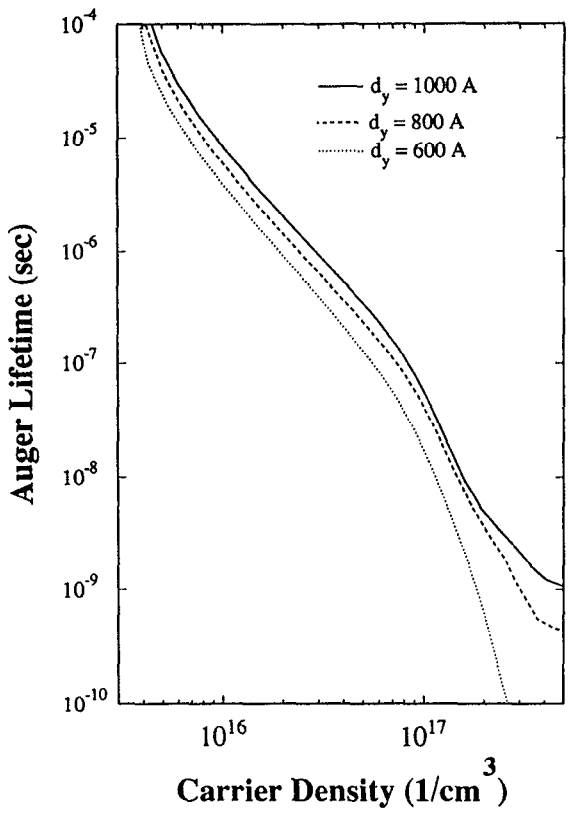

FIG. 5. Auger recombination lifetime in $Hg_{0.85}Cd_{0.15}Te$ QWRs of $d_x = 200$ Å and various values of d_y.

is due to the spikelike density of states in a QWR as illustrated in Ref. 18. The density of states increases with decreasing wire width. Figure 5 shows the Auger recombination lifetime in $Hg_{0.85}Cd_{0.15}Te$ QWRs for various values of the wire width.

It is worthwhile pointing out that the increase in the Auger recombination rate (decrease in the lifetime) is not limited to the CCCH process in HgCdTe but applies to all types of Auger processes and semiconductor materials.

IV. CCCH AUGER RECOMBINATION IN QUANTUM BOXES

In a quantum box with infinitely high barriers, the carriers are confined in the x, y, and z directions, and the eigenfunctions can be written as

$$\phi_{i;m,n,l} = u_{i,k}(\mathbf{r}) \sqrt{\frac{8}{d_x d_y d_z}} \sin(\xi_m x) \sin(\xi_n y) \sin(\xi_l z). \tag{16}$$

The Auger recombination rate per unit volume R_{Aug} ($\mathrm{cm}^{-3}\,\mathrm{s}^{-1}$) can then be written as

$$R_{\mathrm{Aug}} = \frac{2\pi}{\hbar} \frac{1}{(d_x d_y d_z)^3} \sum_{\xi_i} |M_A|^2 P(1,1',2,2') \delta(E_i - E_f), \tag{17}$$

where

$$|M_A|^2 = 4 \left(\frac{4\pi q^2}{\epsilon}\right)^2 \left| \frac{F_{1,1'} F_{2,2'} G_{1,1'}(\xi_x) G_{2,2'}(-\xi_x) G_{1,1'}(\xi_y) G_{2,2'}(-\xi_y) G_{1,1'}(\xi_z) G_{2,2'}(-\xi_z)}{(k_{2'} - k_2)^2 + \xi_x^2 + \xi_y^2 + \xi_z^2 + \lambda^2} \right|^2. \tag{18}$$

In a quantum box, however, $F_{l,l'} = 0$ because the bulk conduction valence-band overlapping is zero at the Γ point. This means that the Auger recombination rate is always zero in a quantum box. However, this argument relies on the validity of the envelope-function model, one band or multiband, in which wave functions are written as products of bulk Bloch functions at the Γ point and the envelope functions [Eq. (16)]. This model has been widely used and proved to be accurate to a great extent.[19] On the other hand, because of the discrete nature of the energy states, it is most likely that $E_i - E_f \neq 0$ and that the delta function in Eq. (16) is zero. Therefore, an Auger process

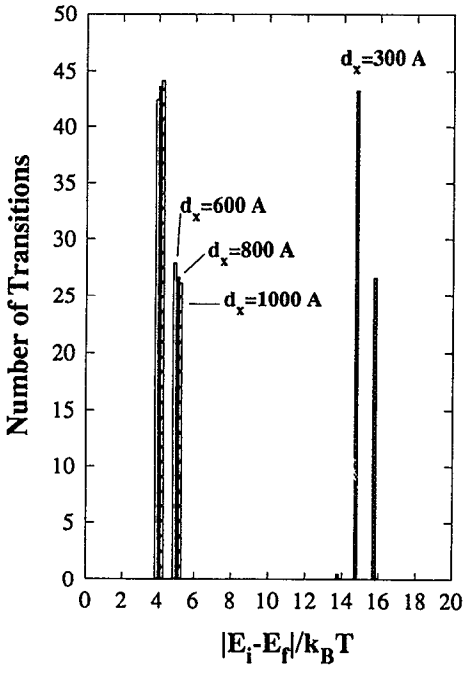

FIG. 6. Number of Auger transitions vs $|E_i - E_f|/k_BT$ for a $Hg_{0.65}Cd_{0.35}Te$ QB with $d_z = 200$ Å and $d_x = d_y = 300$ Å, and a $Hg_{0.85}Cd_{0.15}Te$ QB with $d_z = 200$ Å and $d_x = d_y = 600$ Å, 800 Å, and 1000 Å.

does not occur except in some extremely rare occasions when $E_i - E_f$ happens to be zero for some terms in Eq. (16). Although phonon interactions may broaden the energy levels by an amount $\hbar\omega_{LO} = 10$ meV and induce an Auger process, Fig. 6 shows that most of the transitions have $|E_i - E_f| > 13k_BT$ for a $Hg_{0.65}Cd_{0.35}Te$ QB and $|E_i - E_f| > 3k_BT$ for $Hg_{0.85}Cd_{0.15}Te$ QBs at room temperature, and no Auger process is likely to occur.[20] The energy levels are calculated with the eight-band model outlined in Ref. 18.

V. CONCLUSION

We conclude that the 1-D behavior of quantum-wire structures increases the Auger recombination rate from that of quantum-well structures, whereas Auger recombination is not likely to occur in a quantum-box structure. Therefore, quantum-wire structures are not suitable for long-wavelength lasers. Quantum-box lasers, on the other hand, should exhibit excellent temperature performance and high quantum efficiencies.

ACKNOWLEDGMENT

This work was supported by the Center for Telecommunications Research, by the Joint Services Electronics Program, and by the Naval Research Laboratory. We are grateful to Jill Hacker for useful suggestions.

[1] Y. Horikoshi, in *Semiconductors and Semimetals*, edited by W. T. Tsang (Academic, New York, 1985), Vol. 22C, Chap. 3.
[2] D. L. Partin, IEEE J. Quantum Electron. **QE-24**, 1716 (1988).
[3] A. Ravid, A. Zussman, G. Cinader, and A. Oron, Appl. Phys. Lett. **55**, 2704 (1989).
[4] W. T. Tsang and N. A. Olsson, Appl. Phys. Lett. **43**, 8 (1983).
[5] B. E. A. Saleh and M. C. Teich, *Fundamentals of Photonics* (Wiley, New York, 1991), Chap. 22.
[6] J. P. van der Ziel, T. H. Chiu, and W. T. Tsang, Appl. Phys. Lett. **47**, 1139 (1985); J. P. van der Ziel, T. H. Chiu, and W. T. Tsang, Appl. Phys. Lett. **48**, 315 (1986).
[7] T. C. Harman, J. Electron. Mater. **8**, 191 (1979).
[8] K. K. Mahavadi, J. Bleuse, S. Sivananthan, and J. P. Faurie, Appl. Phys. Lett. **56**, 2077 (1989).
[9] L. C. Chiu and A. Yariv, IEEE J. Quantum Electron. **QE-18**, 1406 (1982).
[10] A. Kastalsky and A. L. Efros, J. Appl. Phys. **69**, 841 (1991).
[11] R. Kubo, *Solid State Physics* (McGraw-Hill, New York, 1969), Chap. II.3.9, p. 358.
[12] M. H. Weiler, in *Semiconductors and Semimetals*, edited by R. K. Willardson and A. C. Beer (Academic, New York, 1980), Vol. 16, Chap. 3.
[13] Y. Jiang, M. C. Teich, and W. I. Wang, J. Appl. Phys. **69**, 6869 (1991).
[14] R. R. Gerhardts, R. Dornhaus, and G. Nimtz, Solid-State Electron. **21**, 1467 (1978).
[15] P. E. Peterson, in *Semiconductors and Semimetals*, edited by R. K. Willardson and A. C. Beer (Academic, New York, 1981), Vol. 18, Chap. 4.
[16] A. R. Beatie and P. T. Landsberg, Proc. Roy. Soc. (London) A **249**, 16 (1959).
[17] J. R. Meyer, Phys. Rev. Lett. **64**, 1963 (1990).
[18] B. E. A. Saleh and M. C. Teich, *Fundamentals of Photonics* (Wiley, New York, 1991), pp. 572–573.
[19] G. Bastard, J. A. Brum, and R. Ferreira, in *Solid State Physics*, edited by H. Ehrenreich and D. Turnbull (Academic, New York, 1991), Vol. 44, p. 229.
[20] H. Sakaki, K. Kato, and H. Yoshimura, Appl. Phys. Lett. **57**, 2800 (1990).